Journal of Information Systems Engineering and Management
2026, 11(3s)
e-ISSN: 2468-4376
https://www.jisem-journal.com/

Research Article

Reliability-Based Design Optimization of Hip Prosthesis Jump Distance: Monte Carlo Analysis of 1,617 Design Configurations

Bouakkar Loubna[1*], Ameddah Hacene[2], Mazouz Hammoudi[1]

[1]*Research Laboratory in Production (LRP), Department of Mechanical Engineering, Faculty of Technology, University of Batna 2 – Mostefa Ben Boulaïd, Batna 05000, Algeria*

[2]*Laboratory of Innovation in Construction, Ecodesign, and Seismic Engineering, Department of Mechanical Engineering, Faculty of Technology, University of Batna 2 – Mostefa Ben Boulaïd, Batna 05000, Algeria*

**Corresponding Author: l.bouakkar@univ-batna2.dz*

ARTICLE INFO

Received: 18 Dec 2024

Revised: 10 Feb 2025

Accepted: 28 Feb 2025

ABSTRACT

This study presents a reliability-based design optimization (RBDO) framework for improving the intrinsic stability of total hip arthroplasty through jump-distance-based design selection. The problem was formulated using four design variables: femoral head diameter, cup abduction angle, cup anteversion angle, and femoral offset. Jump distance (JD) was computed from an analytical geometric model, and uncertainty was propagated by Monte Carlo simulation with 10,000 samples per scenario. A total of 1,617 configurations were evaluated in MATLAB R2020b using parallel computing. The results showed a mean reliability index of 2.3945, with values ranging from -2.9677 to 3.8906, and a mean Monte Carlo jump distance of 12.0659 mm. The best-performing configuration within the explored design space was a 36 mm head, 30° abduction, 30° anteversion, and -2 mm offset, yielding a nominal JD of 20.601 mm, a mean simulated JD of 20.568 mm, and zero failures in 10,000 trials. Parametric analysis showed that abduction angle had the strongest negative influence on reliability, followed by femoral offset, whereas head diameter had a positive effect and anteversion had a weaker but favorable contribution. These results confirm that a probabilistic design framework can discriminate robust from fragile implant configurations more effectively than a purely deterministic threshold check and provide a computationally efficient basis for preclinical implant-orientation optimization.

Keywords: total hip arthroplasty; jump distance; reliability-based design optimization; Monte Carlo simulation; dislocation risk; prosthesis stability

1. INTRODUCTION

Dislocation remains one of the most important complications after total hip arthroplasty (THA), and its occurrence depends on a combination of implant geometry, component orientation, surgical technique, and patient-specific factors. Historically, cup inclination and anteversion were framed through the Lewinnek safe zone, but later studies showed that cup position alone does not fully explain instability, since many dislocated hips are found inside conventional target zones. This has shifted the field toward multifactorial and mechanics-informed stability assessment rather than reliance on a single geometric rule (Lewinnek et al., 1978; Abdel et al., 2016; Seagrave et al., 2017).

Among the available geometric stability indicators, jump distance (JD) is especially attractive because it directly quantifies the lateral translation required for the femoral head to dislocate. Sariali et al. (2009) showed analytically that JD decreases with increasing cup abduction, increases with head diameter, and is strongly affected by offset, making it a concise performance metric for design-oriented stability studies. Large femoral heads have also been

Journal of Information Systems Engineering and Management
2026, 11(3s)
e-ISSN: 2468-4376
https://www.jisem-journal.com/

Research Article

associated clinically with lower dislocation or revision risk, which supports the use of JD as a meaningful surrogate for intrinsic mechanical stability (Kostensalo et al., 2013; Singh & Bhalodiya, 2013; van Steenbergen et al., 2023).

In parallel, reliability-based design optimization has matured as a formal framework for engineering design under uncertainty. Instead of optimizing only nominal performance, RBDO embeds probabilistic constraints or reliability targets into the optimization process, commonly through failure probability P_f or reliability index β. Classical formulations include double-loop, decoupled, and single-loop strategies, with foundational contributions from Hasofer and Lind (1974), Tu et al. (1999), Du and Chen (2004), and Aoues and Chateauneuf (2010).

2. OBJECTIVES

The present work combines these two ideas by applying an RBDO framework to hip-prosthesis jump distance. The objective is not only to identify configurations with high nominal JD, but also to determine which designs remain reliable when plausible geometric and surgical uncertainties are considered. The result is a probabilistic ranking of 1,617 design scenarios, supported by Monte Carlo analysis, statistical synthesis, and multi-dimensional visualization.

3. MATERIALS AND METHODS

3.1 DESIGN VARIABLES AND SEARCH SPACE

Four design variables were considered in the optimization framework: femoral head diameter D (mm), cup abduction angle α (deg), cup anteversion angle ν (deg), and femoral offset o (mm). The nominal design vector was written as:

$$d = [\,D \quad \alpha \quad \nu \quad o\,]^T$$

The design ranges used in the implementation were 28, 32, and 36 mm for head diameter; 30° to 60° in 5° steps for abduction; 0° to 30° in 5° steps for anteversion; and -2 to +3 mm in 0.5 mm steps for offset. The full search space therefore contained 1,617 candidate configurations.

Table 1. *Design variables and search space used in the RBDO framework.*

Parameter	Range	Units	Step size
Head diameter	28–36	mm	4
Abduction angle	30–60	degrees	5
Anteversion angle	0–30	degrees	5
Femoral offset	-2 to +3	mm	0.5

Total combinations: 3 × 7 × 7 × 11 = 1,617.

3.2 DETERMINISTIC JUMP-DISTANCE MODEL

Following the geometric formulation of Sariali et al. (2009), the femoral head radius was defined as:

$$R = D / 2 \quad (1)$$

The planar inclination angle was then written as:

$$\Psi(\alpha, \nu) = \arctan(\tan\alpha \cdot \cos\nu) \quad (2)$$

The corresponding jump distance was calculated by:

$$JD(d) = 2R \cdot \sin[\,(\pi/2 - \Psi(\alpha, \nu) - \arcsin(o/R))\,/\,2\,] \quad (3)$$

Using R = D/2, the expression becomes:

$$JD(d) = D \cdot \sin[\,(\pi/2 - \Psi(\alpha, \nu) - \arcsin(2o/D))\,/\,2\,] \quad (4)$$

This analytical representation makes JD inexpensive to evaluate and therefore well suited to exhaustive design-space exploration. Sariali et al. (2009) also reported that JD decreases as abduction rises, whereas head diameter increases JD and anteversion has a smaller effect than abduction.

Journal of Information Systems Engineering and Management
2026, 11(3s)
e-ISSN: 2468-4376
https://www.jisem-journal.com/

Research Article

3.3 PROBABILISTIC MODEL AND UNCERTAINTY PROPAGATION

To account for variability in implantation and geometry, the realized variables were modeled as independent normal random variables:

$$X = [\ D_r \quad \alpha_r \quad \nu_r \quad o_r\ ]^T \quad (5)$$

with the following standard deviations:

$$D_r \sim \mathcal{N}(D, \sigma\_D^2), \quad \sigma\_D = 1.5 \text{ mm} \quad (6)$$

$$\alpha_r \sim \mathcal{N}(\alpha, \sigma\_\alpha^2), \quad \sigma\_\alpha = 3° \quad (7)$$

$$\nu_r \sim \mathcal{N}(\nu, \sigma\_\nu^2), \quad \sigma\_\nu = 2° \quad (8)$$

$$o_r \sim \mathcal{N}(0, \sigma\_o^2), \quad \sigma\_o = 1 \text{ mm} \quad (9)$$

The stochastic jump distance was therefore evaluated as:

$$JD(X) = D_r \cdot \sin [\ (\ \pi/2 - \Psi(\alpha_r, \nu_r) - \arcsin(2o_r/D_r)\ )\ /\ 2\ ] \quad (10)$$

Monte Carlo simulation with 10,000 samples was executed for each scenario to quantify uncertainty propagation across the design space.

3.4 RELIABILITY FORMULATION AND OPTIMIZATION PROBLEM

The required minimum jump distance was fixed at 8 mm. The limit-state function was defined as:

$$g(X) = JD(X) - JD\_req \quad (11)$$

Failure occurs when:

$$g(X) \le 0 \quad \Leftrightarrow \quad JD(X) < 8 \text{ mm} \quad (12)$$

The failure probability was estimated as:

$$P\_f(d) = P[\ g(X) \le 0\ ] \quad (13)$$

$$\hat{P}\_f(d) = (1/N)\ \Sigma\ I(\ g(X^{(i)}) \le 0\ ) \quad (14)$$

The reliability index was then calculated from the standard normal inverse cumulative distribution function:

$$\beta(d) = -\ \Phi^{-1}(\ P\_f(d)\ ) \quad (15)$$

The optimization problem was posed as:

$$d^* = \arg\max \beta(d) \quad (16)$$

subject to the minimum geometric stability requirement:

$$JD(d) \ge 8 \text{ mm} \quad (17)$$

Equivalently, the problem can be expressed as the minimization of the failure probability over the admissible design space.

3.5 COMPUTATIONAL WORKFLOW

The framework was implemented in MATLAB R2020b and comprised four main stages: (i) full design-space enumeration of the 1,617 candidate scenarios, (ii) parallel Monte Carlo reliability analysis using MATLAB's Parallel Computing Toolbox, (iii) statistical analysis of the resulting reliability and jump-distance distributions, and (iv) multi-dimensional visualization for design-space interpretation. In the reported run, the analysis used four workers and completed in 5.36 s, corresponding to approximately 3.317 ms per scenario.

a. Design space enumeration: systematic exploration of all 1,617 combinations.
b. Parallel computing: parfor-based evaluation to reduce runtime.
c. Statistical analysis: global summaries, grouped means, and correlation analysis.

Journal of Information Systems Engineering and Management
2026, 11(3s)
e-ISSN: 2468-4376
https://www.jisem-journal.com/

Research Article

d. Visualization: histograms, 3D scatter plots, bubble plots, heat maps, and main-effects curves.

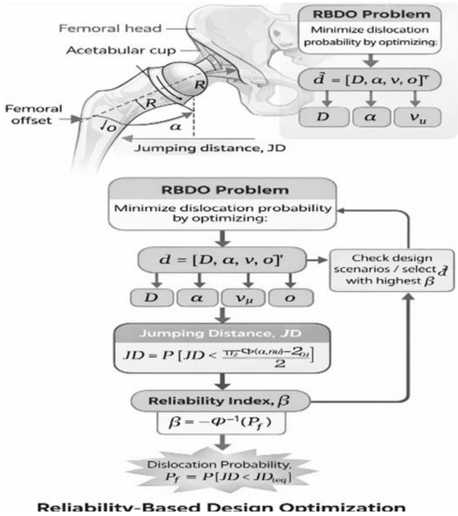

4. RESULTS & DISCUSSION

4.1. GLOBAL STATISTICAL SUMMARY

The global output of the Monte Carlo-based RBDO study is summarized in Table 2. The mean reliability index over the full design space was 2.3945, with a broad spread from -2.9677 to 3.8906. The mean nominal JD and mean Monte Carlo JD were 12.0747 mm and 12.0659 mm, respectively, indicating that the analytical response remains stable under the adopted uncertainty amplitudes.

Table 2. Global performance summary of the 1,617 simulated designs.

Metric	Value
Total scenarios	1,617
Monte Carlo samples per scenario	10,000
Total runtime	5.36 s
Average runtime per scenario	3.317 ms
Mean reliability index, β	2.3945
Standard deviation of β	1.6658
Minimum β	-2.9677
Maximum β	3.8906
Mean nominal JD	12.0747 mm
Mean Monte Carlo JD	12.0659 mm
Designs with nominal JD ≥ 8 mm	1,433 / 1,617
Designs with β ≥ 2.0	1,042 / 1,617

Two observations emerge immediately. First, the very small difference between the nominal and Monte Carlo mean JD values suggests limited bias introduced by uncertainty propagation at the global level. Second, the number of designs satisfying the deterministic threshold JD ≥ 8 mm (1,433) is substantially larger than the number achieving β ≥ 2.0 (1,042), showing that deterministic feasibility alone overestimates the number of robust solutions.

Journal of Information Systems Engineering and Management
2026, 11(3s)
e-ISSN: 2468-4376
https://www.jisem-journal.com/
Research Article

4.2. BEST-RANKED CONFIGURATION

The highest-ranked design found in the explored space is presented in Table 3. It combined the largest head diameter with the lowest abduction and the most favorable offset level in the adopted formulation. The result is mechanically coherent because larger heads increase the dislocation-free travel, lower abduction preserves jump distance, and lower offset reduces the geometric penalty introduced by the analytical model.

Table 3. Best-ranked design configuration within the explored search space.

Parameter	Value
Head diameter	36 mm
Abduction angle	30°
Anteversion angle	30°
Femoral offset	-2 mm
Nominal JD	20.601 mm
Monte Carlo mean JD	20.568 mm
JD standard deviation	1.3647 mm
JD minimum	15.365 mm
JD maximum	25.808 mm
Number of failures	0 / 10,000
P_f	0
β	3.8906

A technical point is important here. The maximum reliability index of 3.8906 corresponds to the finite-sample ceiling induced by the Monte Carlo implementation, because zero observed failures were clamped in the code to a non-zero lower probability bound. Consequently, several zero-failure designs are effectively tied at the same reliability ceiling, and finer discrimination among the best-performing solutions would require a larger sample size or a dedicated reliability method such as FORM, SORM, or importance sampling.

$$\beta\_{max,MC} = -\Phi^{-1}(0.5 / N) \approx 3.8906 \text{ for } N = 10{,}000 \quad (18)$$

4.3. MAIN EFFECTS OF DESIGN VARIABLES

Grouped statistical analysis revealed strong and clearly interpretable trends for the four design variables. Table 4 reports the main-effect changes from the lowest to the highest level of each parameter.

Table 4. Main-effect summary from grouped results.

Variable	Lowest / first level	Highest / last level	Change in mean JD	Change in mean β	Interpretation
Diameter	28 mm	36 mm	+29.97%	+71.41%	Larger heads strongly improve robustness
Abduction	30°	60°	-48.64%	-97.77%	Strongest adverse effect
Anteversion	0°	30°	+8.43%	+19.53%	Secondary but favorable effect
Offset	-2 mm	+3 mm	-32.27%	-67.86%	Strong negative effect when increased

Journal of Information Systems Engineering and Management
2026, 11(3s)
e-ISSN: 2468-4376
https://www.jisem-journal.com/

Research Article

Abduction angle exerted the strongest influence on both JD and β. Increasing abduction from 30° to 60° reduced mean JD from 15.831 mm to 8.130 mm and collapsed mean β from 3.793 to 0.085. Head diameter had the strongest beneficial effect, increasing mean β from 1.733 at 28 mm to 2.970 at 36 mm. Anteversion produced a smaller but favorable increase in both JD and reliability, whereas offset showed a strong monotonic penalty in the current formulation.

4.4. CORRELATION ANALYSIS

Table 5. Pearson correlations with reliability index and nominal jump distance.

Variable	Corr. with β	Corr. with nominal JD
Diameter	+0.3034	+0.3945
Abduction	-0.7491	-0.7900
Anteversion	+0.0888	+0.1012
Offset	-0.4418	-0.4493

The correlation analysis reinforces the main-effect results. Abduction dominated the reliability response, followed by offset. Diameter had a moderate positive contribution, whereas anteversion remained weakly positive. This ranking is important because it shows that not all variables deserve the same optimization priority in a practical preoperative or implant-design workflow.

3.5. FIGURE-BASED ANALYSIS OF THE DESIGN SPACE

Figures 1 to 7 summarize the structure of the explored design space. The histograms highlight the global spread of reliability and jump distance, the 3D scatter and bubble plot reveal the clustering of robust designs, the heat maps identify locally optimal subregions, and the main-effects plot condenses the dominant parametric trends.

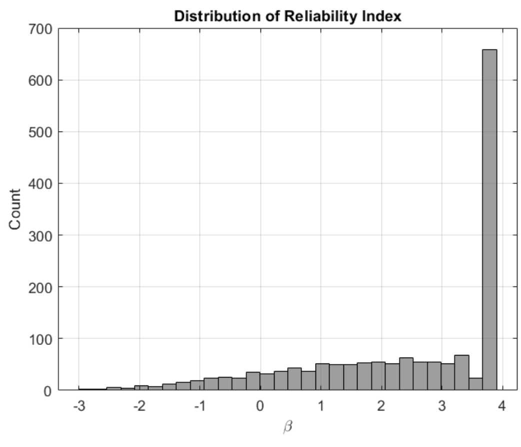

Figure 1. Distribution of the reliability index β across the 1,617 design scenarios.

The reliability histogram is highly right-skewed, with a prominent terminal spike near β ≈ 3.89. This spike corresponds to zero-failure solutions that reach the Monte Carlo reliability ceiling imposed by the finite sample size.

Journal of Information Systems Engineering and Management
2026, 11(3s)
e-ISSN: 2468-4376
https://www.jisem-journal.com/

Research Article

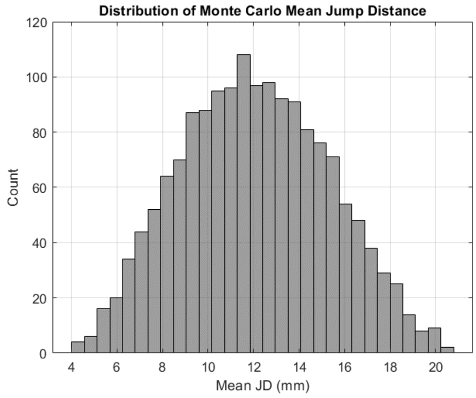

Figure 2. Distribution of the Monte Carlo mean jump distance across the full design space.

The mean JD distribution is approximately unimodal and centered around 12 mm, with a broad spread from about 4 mm to above 20 mm. This indicates that the design space contains both clearly unsafe and highly robust regions.

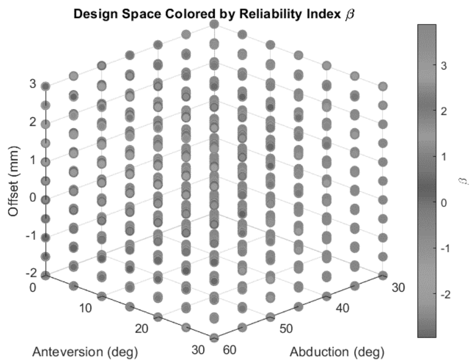

Figure 3. Three-dimensional design space colored by reliability index β.

High reliability clusters at low abduction, larger diameter, and negative-to-small offset. Anteversion shifts reliability upward, but the effect is visually weaker than that of abduction and offset.

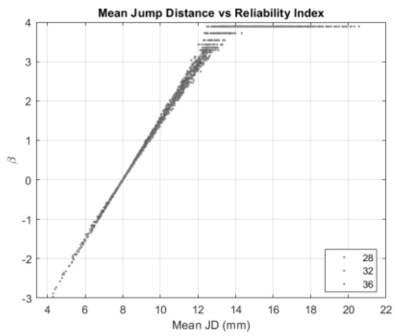

Figure 4. Mean jump distance versus reliability index, grouped by femoral head diameter.

The near-linear trend between mean JD and β indicates that configurations with larger geometric safety margins almost always exhibit better reliability. The flattening at the top reflects the finite-sample β ceiling.

Journal of Information Systems Engineering and Management
2026, 11(3s)
e-ISSN: 2468-4376
https://www.jisem-journal.com/

Research Article

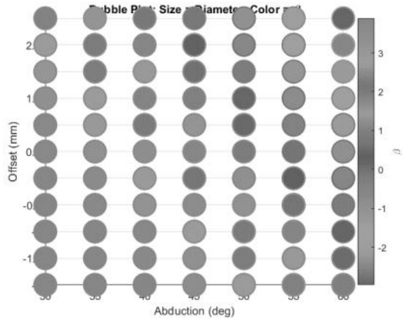

Figure 5. Bubble plot in the abduction–offset plane, with bubble size representing diameter and color representing reliability index β.

The plot emphasizes the joint penalty of large abduction and large positive offset. Even larger diameters cannot fully compensate for the reliability loss in the upper-right region of the design map.

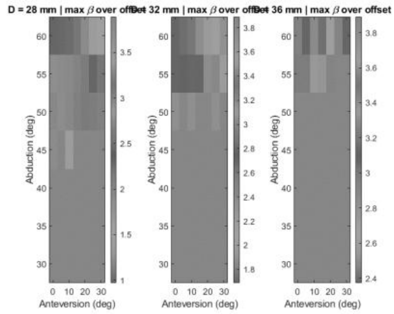

Figure 6. Heat maps of the maximum reliability index β over offset for each diameter level.

For all three diameters, the best regions are concentrated at low abduction. Increasing diameter expands the high-β region, confirming that larger heads improve robustness across a wider range of orientations.

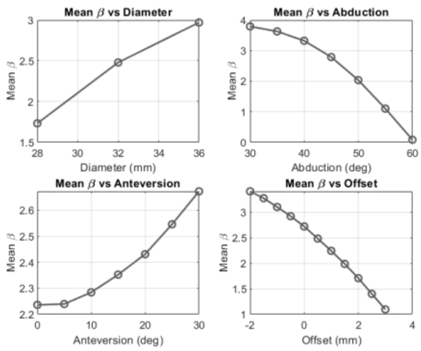

Figure 7. Main-effects plots of the mean reliability index versus each design variable.

Diameter and anteversion increase mean reliability, whereas abduction and offset reduce it. The abduction curve is the steepest, confirming that this variable dominates the reliability response.

5. DISCUSSION

The present results support three central conclusions. First, JD-based optimization under uncertainty is feasible at very low computational cost when an analytical geometric model is available. Second, probabilistic analysis is more selective than deterministic threshold screening. Third, the ranking of influential variables is not symmetric: abduction dominates, offset is strongly penalizing, diameter is clearly beneficial, and anteversion is secondary.

The result that larger head diameters improve reliability is fully consistent with prior biomechanical and clinical evidence. Sariali et al. (2009) mathematically linked larger heads to increased jump distance, while registry and cohort studies found lower dislocation-related revision rates with larger heads, particularly up to 36 mm (Kostensalo et al., 2013; Singh & Bhalodiya, 2013; van Steenbergen et al., 2023).

The dominant adverse effect of abduction also fits the literature. The original jump-distance formulation explicitly predicts JD loss with increased cup abduction, and broader reviews have shown that cup position remains relevant even though it is not, by itself, a sufficient explanation of instability (Sariali et al., 2009; Seagrave et al., 2017).

At the same time, the study should not be interpreted as proposing a universal surgical prescription such as 30° abduction and 30° anteversion for all patients. Modern evidence shows that many dislocations occur inside classic cup-position safe zones, indicating that instability is multifactorial and influenced by soft tissues, spinopelvic motion, combined anteversion, surgical approach, and patient anatomy (Abdel et al., 2016; van Erp et al., 2021).

The offset result deserves careful interpretation. In the present geometric JD formulation, more positive offset reduces JD and therefore reduces reliability. However, clinical studies have also shown that restoring femoral offset can be important for soft-tissue tension, stability, and function. This means that a pure JD metric captures one important stability mechanism, but not the entire biomechanical picture. A clinically complete optimization should therefore combine JD with impingement-free range of motion, soft-tissue tension, muscle moment arms, and patient-specific anatomy (Forde et al., 2018; Hu et al., 2021).

Methodologically, the present framework has several strengths: exhaustive exploration of the discrete design space, explicit uncertainty propagation, fast runtime, and clear parametric interpretability. Its main limitations are equally clear: the uncertainty variables were assumed independent and normally distributed; the model is purely geometric and does not include contact, soft tissue, or impingement mechanics; and the zero-failure plateau at $\beta = 3.8906$ limits discrimination among the very best designs. These limitations do not invalidate the framework, but they define its current scope as a fast pre-screening and decision-support tool rather than a complete patient-specific dislocation simulator.

6. CONCLUSION

A complete Monte Carlo-based RBDO analysis of hip-prosthesis jump distance was performed over 1,617 configurations using four design variables. The framework identified a clear reliability hierarchy within the design space and showed that deterministic feasibility is insufficient to distinguish robust from marginal solutions. The best design in the explored space was a 36 mm head, 30° abduction, 30° anteversion, and -2 mm offset, with a nominal JD of 20.601 mm, a mean simulated JD of 20.568 mm, and zero failures in 10,000 samples.

The most important design insight is that abduction angle is the dominant destabilizing factor, followed by offset, whereas head diameter is the strongest stabilizing factor and anteversion has a smaller positive role. These findings are consistent with the analytical jump-distance literature and broadly compatible with the clinical evidence favoring larger heads and careful restoration of hip biomechanics.

From an engineering perspective, the proposed workflow is attractive because it is transparent, fast, and scalable. From a clinical perspective, it should be interpreted as a geometric-probabilistic optimization layer that complements, rather than replaces, more comprehensive patient-specific stability assessment. Future work should integrate impingement, soft-tissue constraints, spinopelvic kinematics, and possibly surrogate-based or FORM-assisted reliability methods to refine ranking among high-reliability designs.

REFERENCES

[1] Abdel, M. P., von Roth, P., Jennings, M. T., Hanssen, A. D., & Pagnano, M. W. (2016). What safe zone? The vast majority of dislocated THAs are within the Lewinnek safe zone for acetabular component position. Clinical Orthopaedics and Related Research, 474(2), 386–391. https://doi.org/10.1007/s11999-015-4432-5

[2] Aoues, Y., & Chateauneuf, A. (2010). Benchmark study of numerical methods for reliability-based design optimization. Structural and Multidisciplinary Optimization, 41(2), 277–294. https://doi.org/10.1007/s00158-009-0412-2

[3] Du, X., & Chen, W. (2004). Sequential optimization and reliability assessment for probabilistic design. Journal of Mechanical Design, 126(2), 225–233. https://doi.org/10.1115/1.1649968
[4] Forde, B., Engeln, K., Bedair, H., Yacovelli, S., Greene, M., Bragdon, C., & Freiberg, A. (2018). Restoring femoral offset is the most important technical factor in preventing total hip arthroplasty dislocation. Journal of Orthopaedics, 15(1), 131–133. https://doi.org/10.1016/j.jor.2018.01.026
[5] Hasofer, A. M., & Lind, N. C. (1974). Exact and invariant second-moment code format. Journal of the Engineering Mechanics Division, 100(1), 111–121. https://doi.org/10.1061/JMCEA3.0001848
[6] Hu, X., Li, Q., Chen, J., Cheng, L., Hu, Y., Yang, J., & Wang, Q. (2021). Optimizing the femoral offset for restoring physiological hip muscle function in total hip arthroplasty. Frontiers in Bioengineering and Biotechnology, 9, 645019. https://doi.org/10.3389/fbioe.2021.645019
[7] Kostensalo, I., Junnila, M., Virolainen, P., Remes, V., Matilainen, M., & Eskelinen, A. (2013). Effect of femoral head size on risk of revision for dislocation after total hip arthroplasty. Acta Orthopaedica, 84(4), 342–347. https://doi.org/10.3109/17453674.2013.810518
[8] Lewinnek, G. E., Lewis, J. L., Tarr, R., Compere, C. L., & Zimmerman, J. R. (1978). Dislocations after total hip-replacement arthroplasties. The Journal of Bone and Joint Surgery. American Volume, 60(2), 217–220.
[9] Sariali, E., Lazennec, J. Y., Khiami, F., & Catonné, Y. (2009). Mathematical evaluation of jumping distance in total hip arthroplasty: Influence of abduction angle, femoral head offset, and head diameter. Acta Orthopaedica, 80(3), 277–282. https://doi.org/10.3109/17453670902988378
[10] Seagrave, K. G., Troelsen, A., Malchau, H., Husted, H., & Gromov, K. (2017). Acetabular cup position and risk of dislocation in primary total hip arthroplasty: A systematic review of the literature. Acta Orthopaedica, 88(1), 10–17. https://doi.org/10.1080/17453674.2016.1251255
[11] Singh, S. P., & Bhalodiya, H. P. (2013). Head size and dislocation rate in primary total hip arthroplasty. Indian Journal of Orthopaedics, 47(5), 443–448. https://doi.org/10.4103/0019-5413.118198
[12] Tu, J., Choi, K. K., & Park, Y. H. (1999). A new study on reliability-based design optimization. Journal of Mechanical Design, 121(4), 557–564. https://doi.org/10.1115/1.2829499
[13] van Erp, J. H. J., van der Wal, B. C. H., van den Bekerom, M. P. J., & Pijls, B. G. (2021). The role of the femoral component orientation on dislocations in total hip arthroplasty: A systematic review. Archives of Orthopaedic and Trauma Surgery, 141, 699–717. https://doi.org/10.1007/s00402-020-03638-4
[14] van Steenbergen, L. N., de Steiger, R. N., Crawford, R. W., Noorduyn, J. C. A., Nelissen, R. G. H. H., & Poolman, R. W. (2023). Femoral head size and surgical approach affect dislocation and overall revision rates in total hip arthroplasty: Up to 9-year follow-up data of 269,280 procedures in the Dutch Arthroplasty Register. HIP International, 33(6), 1056–1062. https://doi.org/10.1177/11207000231160223